An Analysis of a Set of Creep-Strain-Rate and Time-to-Creep Fracture Data for a 9Cr-1Mo-0.2V Steel

J. Čadek and V. Šustek

Institute of Physics of Materials
Academy of Sciences of the Czech Republic
616 62 Brno, Czech Republic

ABSTRACT

In the present paper, a remarkably extensive set of creep and creep fracture data for a 9Cr-1Mo-0.2V (P91 type) stainless steel published by Sklenička and collaborators /1/ are re-analysed in an attempt to account for an unusual stress and temperature dependence of both the creep strain rate and the time to creep fracture. The analysis suggests strongly that (i) the creep strain rate is not recovery controlled, (ii) neither is the creep strain rate controlled by dislocation climb around carbide particles provided no interaction of dislocations with carbide particles takes place and finally (iii) the Rösler -Arzt model assuming an attractive interaction of dislocations with dispersed particles and thermally activated detachment of the dislocations from the particles fails to account for the creep data of interest.

It is suggested that the carbide particles play an indirect role affecting the development of dislocation substructure in the course of creep and, especially, the effect of stress and temperature on its parameters. This is in accord with the original data interpretation by Sklenička and his collaborators /1/.

Everything that holds for the creep strain rate essentially holds for the time to creep fracture as well. In fact, the time to creep fracture is most probably controlled by the same process and/or mechanism as creep in the 9Cr-1Mo-0.2V (P91 type) steel, as originally suggested by Sklenička *et al.* /1/.

1. INTRODUCTION

At the present time, it is widely believed that 9% Cr steels with significantly improved creep properties will find important applications in advanced power engineering. This is why the fundamental aspects of creep and creep fracture of these steels have become of considerable interest since the early nineties.

Recently, Sklenička *et al.* /1/ presented an extensive study of creep behaviour and microstructure of a 9%Cr-1%Mo-0.2%V (P91 type) steel. The authors used the isothermal constant stress creep test technique, performed the creep tests in purified argon and measured minimum creep strain rates at five temperatures ranging from 823K to 923K. The testing temperatures were controlled to within IK, the strains were measured using linear variable differential transformers (LVDT). The outputs of the LVDT were computer processed.

The measured minimum creep strain rates covered six orders of magnitude and the same holds for the measured times to creep fracture. But, especially, the authors /1/ attempted to correlate some creep properties with the evolution of dislocation structure consisting of subgrains and free dislocations within subgrains. Although the area fraction of carbide particles amounted to about 0.065 in crept specimens, the authors concluded that "the effect of the rearrangement of dislocations and subgrain coarsening on creep is more important than the effect of precipitation hardening".

In the present paper, minimum creep strain rate and time to creep fracture data published by Sklenička *et al.* /1/ are re-analysed with the aim:

1) to find out whether the minimum creep strain rate as well as the time to creep fracture of the steel under consideration is lattice diffusion controlled, and
2) to attempt to identify the role of carbide particles in creep and creep fracture of this steel without further extending the dislocation structure investigation performed by Sklenička *et al.* /1/.

2. MINIMUM CREEP STRAIN RATE

2.1. Applied Stress and Temperature Dependence

In Fig. 1, the minimum creep strain rates $\dot{\varepsilon}_m$ are plotted against applied stresses σ for five various temperatures ranging from 823 K to 923 K using the data presented by Sklenička *et al.* /1/. From these relations, the apparent stress exponent

$$m_c = [(\partial \ln \dot{\varepsilon}_m) / (\partial \ln \sigma)]_T \qquad (1)$$

and the apparent activation energy of creep

$$Q_c = [(\partial \ln \dot{\varepsilon}_m) / (\partial(-1/RT)]_T \qquad (2)$$

were obtained. In eqns. (1) and (2), T is the temperature and R is the gas constant.

From Fig. 2 it can be seen that the exponent m_c decreases with increasing temperature approximately linearly from a value close to 17 at 823 K to a value close to 10 at 923 K (c.f. Ref. /1/). Accordingly (see e.g. Ref. /2/), the activation energy Q_c decreases with increasing stress; thus Q_c decreases from a value close to 850 kJ mol^{-1} at σ = 100 MPa, to a value of about 350 kJmol^{-1} at σ = 400 MPa, Fig. 3. The apparent activation energy Q_c is much higher than the activation enthalpy of lattice diffusion ΔH_L estimated /3/ to 237 kJmol^{-1}. Because of the high values and the strong stress dependence of Q_c, the difference between Q_c and ΔH_L cannot be accounted for by the temperature dependence of the shear modulus G. This follows from Fig. 4, in which the minimum creep strain rates normalized to the coefficient of lattice diffusion D_L [m^{2}s^{-1}] = 1.8 x 10^4 exp[–237/RT] (see Ref. /3/) are plotted against the applied stress normalized to the shear modulus G[MPa]

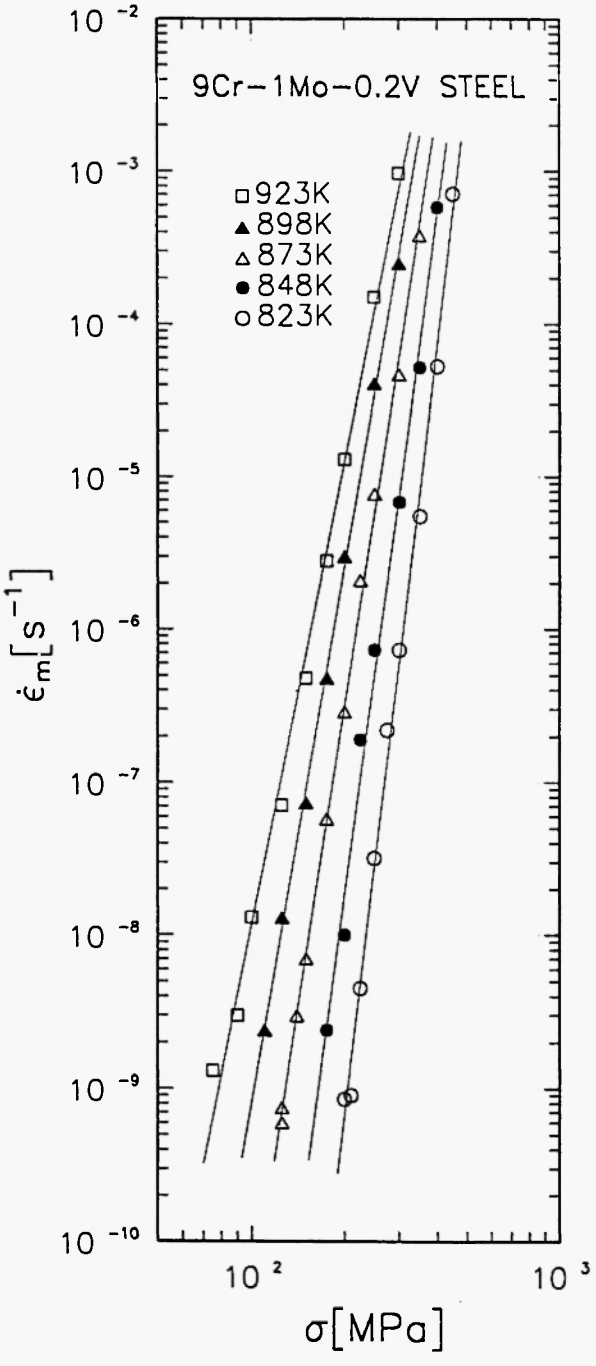

Fig. 1: Applied stress dependence of minimum creep strain rate for five temperatures in an interval 823K - 923K. Data of Sklenička *et al.* /1/.

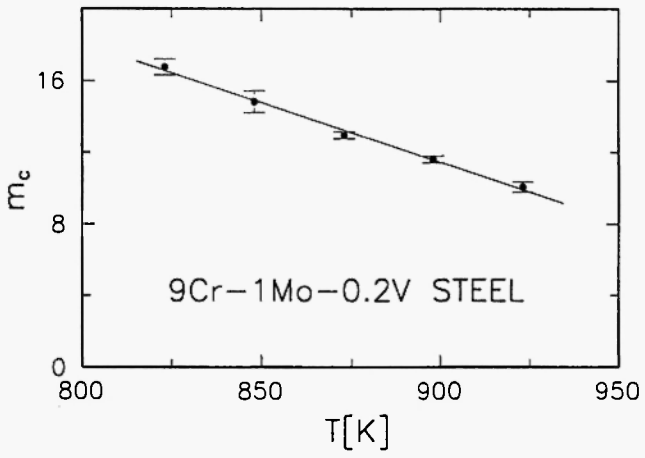

Fig. 2: Temperature dependence of the apparent stress exponent m_c. This exponent does not depend on applied stress σ and can be described as $m_c = 505497/T-44.75$.

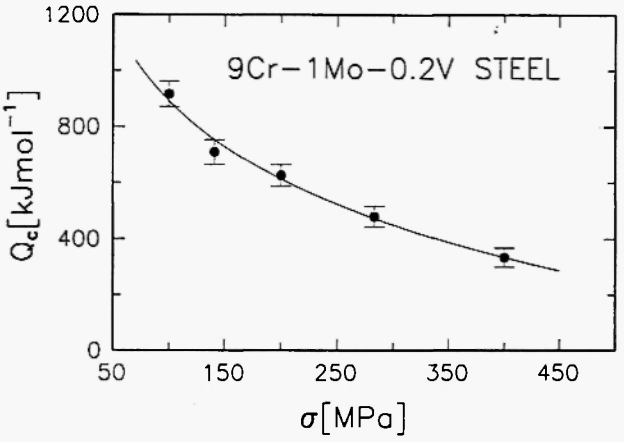

Fig. 3: Stress dependence of the apparent activation energy of creep Q_c. The energy Q_c does not depend on temperature and can be described as Q_c [kJmol^{-1}] = 2744.9-402.41nσ.

= 97400–0.039T /3/. In this figure, the data points cannot be fitted by a single straight line; only the straight line for a temperature of 873K is shown. Hence, Fig. 4 suggests, quite strongly, that the minimum creep strain rate is not lattice diffusion controlled. Consequently, the question of possible creep strain rate controlling process becomes very urgent.

In fact, the recovery involving climb and annihilation of free dislocations, which in itself depends on lattice diffusion, cannot in all probability account for the creep strain rate behaviour of the steel of interest. The same applies to dislocation climb past carbide

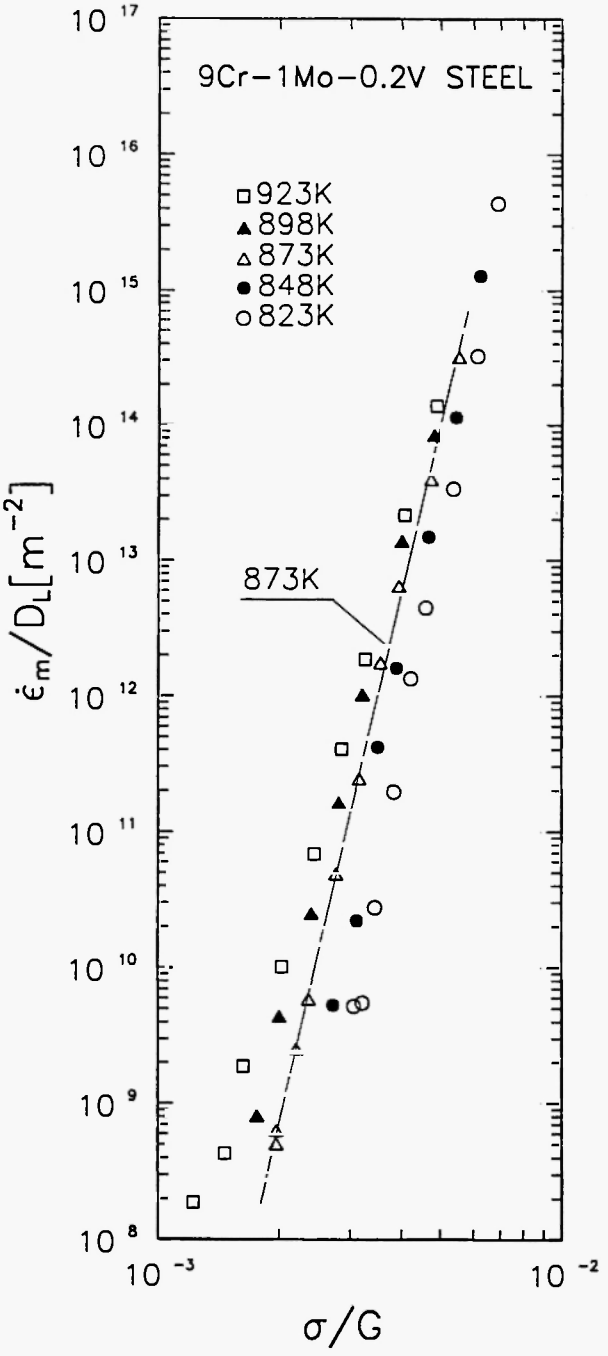

Fig. 4: The minimnm creep strain rates normalized to the lattice diffusion coefficient, plotted against stress normalized to the shear modulus, σ/G. The data points do not fit a single curve; in the figure, only the curve for 873K is shown.

particles, provided the dislocations do not exhibit an attractive interaction with these particles /4/.

However, the carbides of $M_{23}C_6$ type are certainly not coherent with the matrix. Hence, an attractive interaction of dislocation with these particles may, in principle, be expected /5/. Then, the dislocation climb around a particle can be relatively easy as compared to the detachment of the dislocation from the particle after the climb around it has been finished. The shear stress τ_d necessary to detach dislocations from "interacting" particles is, of course, higher than the applied stress τ and is expressed as /5/:

$$\tau_d = \tau_0 (1 - k_R^2)^{1/2} \quad (3)$$

where τ_O is the Orowan bowing stress and k_R is the relaxation factor characterizing the "strength" of dislocation/particle interaction ($0 \le k_R \le 1$) /5/. The factor k_R cannot be calculated from the first principles at the present time. However, it can be estimated from the creep data of interest applying the creep model proposed by Rösler and Arzt /6/. The same holds for the detachment stress τ_d as well as for the activation energy of detachment E_d. The model is based on the realistic assumption that the process of dislocation detachment from particles is thermally activated.

3. IS THE CREEP IN THE 9Cr-1Mo-0.2V STEEL CONTROLLED BY THERMALLY ACTIVATED DETACHMENT OF DISLOCATIONS FROM CARBIDE PARTICLES?

Rösler and Arzt /6/ developed the following equation for the activation energy of detachment of dislocations from particles:

$$E_d = Gb^2r[(1-k_R)(1-\tau/\tau_d)]^{3/2} \quad (4)$$

where r is the particle radius. This equation is a principal one for the model. The creep equation is then written as:

$$\dot{\varepsilon}/D_L = (6\rho\lambda/b) \exp[-E_d/kT] \quad (5)$$

where λ is the half interparticle spacing, ρ the density of mobile dislocations, b the length of Burgers vector and k the Boltzmann constant. $C = 6\rho\lambda/b$ is called "structure factor" in the following, independently of whether it is deduced from creep data or estimated using the structure data as ρ, λ and b.

Combining eqns. (1), (4) and (5) and neglecting the stress dependence of the structure factor C in the latter equation, the expression for the apparent stress exponent m_c is obtained, from which the following expression for k_R follows:

$$k_R = 1 - [(2kT/3Gb^2r)\, m_c / (1 - \sigma/\sigma_d)^{1/2} (\sigma/\sigma_d)]^{2/3} \quad (6)$$

Combining eqns. (2), (4) and (5) the expression for σ/σ_d can be written as

$$\sigma/\sigma_d = [3(Q_c - \Delta H_L)/ 2RTm_c (1 - T\, dG/ dT) +1]^{-1} \quad (7)$$

In eqns. (6) and (7) the normal stress σ was introduced instead of the shear stress τ.

Now, k_R and σ_d can be estimated using eqns.(6) and (7), since the quantities m_c and Q_c are known from experiment as the functions of temperature and applied stress, respectively, and the mean "equivalent" particle diameter 2r can be taken from the paper by Sklenička *et al.* /1/: 2r = 27.3 nm.

Since the apparent stress exponent m_c depends strongly on temperature (Fig. 2) and the apparent activation energy Q_c depends strongly on applied stress (Fig. 3), the following procedure was chosen: First, the values of applied stress causing the normalized minimum creep strain rates $\dot{\varepsilon}_m / D_L$ equal to 5×10^9 m^{-2} and $5 \times 10^{11} m^{-2}$ were determined by interpolation from the $\dot{\varepsilon}_m / D_L$ vs σ/G relations (Fig. 4) for every temperature under consideration. Thus, for instance, for a temperature 873 K, the stress σ causing the normalized minimum creep strain rate $\dot{\varepsilon}_m / D_L = 5 \times 10^9$ m^{-2} is equal to 147.2 MPa. Second, the detachment stress σ_d and the relaxation factor k_R were calculated for every temperature and applied stress corresponding to the respective temperature.

Relations between applied stress σ causing the strain rates $\dot{\varepsilon}_m / D_L$ equal to $5 \times 10^9 m^{-2}$ and $5 \times 10^{11} m^{-2}$, respectively, and temperature are shown in Fig. 5. Relations between the ratio of applied stress σ and detachment stress σ_d, i.e. σ/σ_d, and temperature for the values of $\dot{\varepsilon}_m / D_L$ under consideration are presented in Fig. 6. Further, the respective relations between the re-

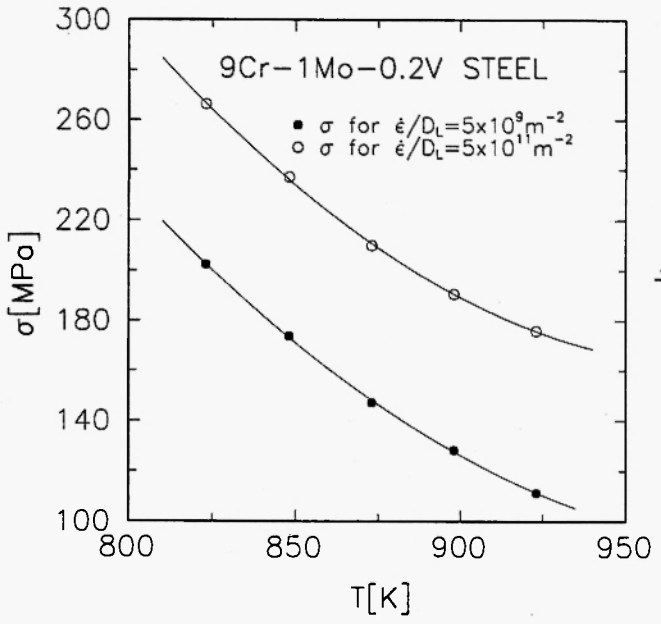

Fig. 5: Relations between applied stress σ causing the strain rates $\dot{\varepsilon}_m / D_L$ equal to 5×10^9 m^{-2} and 5×10^{11} m^{-2} respectively, and temperature.

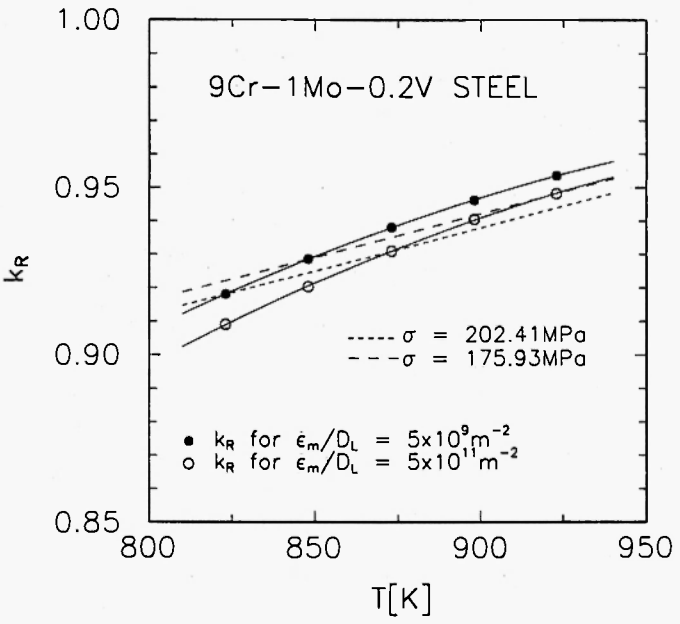

Fig. 7: Relations between relaxation factor k_R and temperature for $\dot{\varepsilon}_m / D_L$ equal to 5×10^9 m^{-2} and 5×10^{11} m^{-2}.

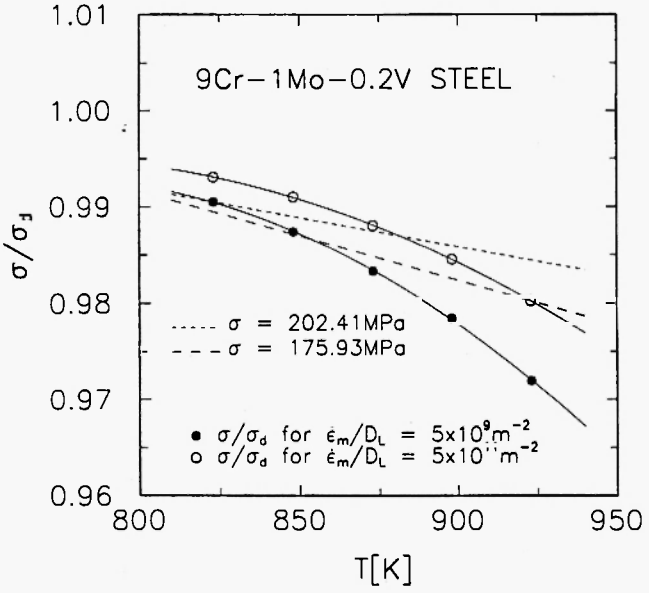

Fig. 6: Relations between the ratio of applied stress σ and detachment stress σ_d, i.e. σ/σ_d and temperature for the $\dot{\varepsilon}_m / D_L$ values under consideration.

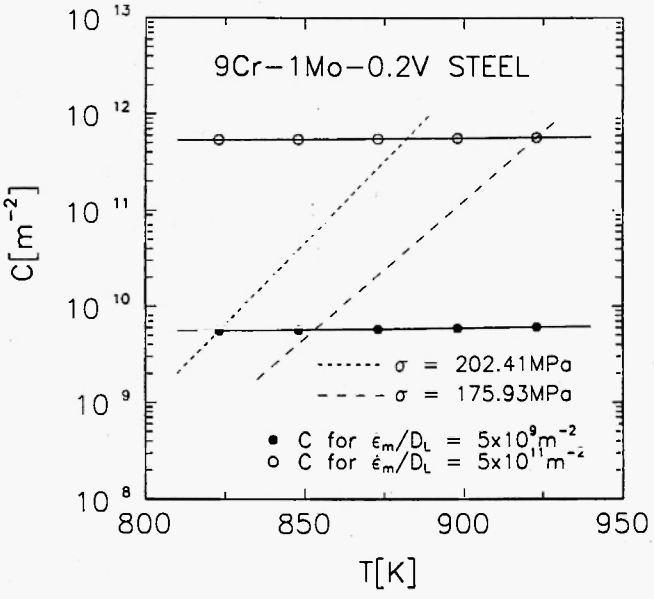

Fig. 8: The structure factor C obtained from creep data plotted against temperature for the $\dot{\varepsilon}_m / D_L$ values under consideration (see Fig. 7).

laxation factor k_R and temperature are shown in fig. 7 and, finally, the relations between the structure factor C = 6 $\lambda\rho/b$ and temperature are presented in Fig. 8. The values of σ_d, k_R and C were calculated by means of eqns. (7), (6) and (5), respectively. From the results of calculation, the following conclusions can be drawn:

(i) The detachment stress σ_d increases with decreasing temperature, the σ_d/σ ratio is close to 1, Fig. 6. For instance, at 873 K σ_d/σ = 0.983 for $\dot{\varepsilon}_m / D_L = 5 \times 10^9 m^2$ and 0.988 for $\dot{\varepsilon}_m / D_L = 5 \times 10^{11} m^{-2}$.

(ii) The relaxation factor increases with increasing temperature, its value seems to be quite reasonable even at 923 K. For $\dot{\varepsilon}_m / D_L = 5 \times 10^9 m^{-2}$ the values of k_R are slightly greater than those for $\dot{\varepsilon}_m / D_L = 5 \times 10^{11} m^{-2}$ (Fig. 6).

(iii) The structure factor C does not depend on temperature significantly for any of the two values of $\dot{\varepsilon}_m / D_L$; however, for $\dot{\varepsilon}_m / D_L = 5 \times 10^9 m^{-2}$ it is smaller than that for the $\dot{\varepsilon}_m / D_L = 5 \times 10^{11} m^{-2}$ (Fig. 7). The values of C presented in Fig. 8 can be compared with that calculated from the structure data, estimating the half interparticle spacing by means of the relation $\lambda = (f^{1/3} - 1)r$, where the volume fraction of carbide particles f and the mean particle radius r were estimated from the data published by Sklenička *et al.* /1/, similarly to the average mobile dislocation density $\rho = 8.6 \times 10^{13} m^{-2}$. In this way, the structure factor C was estimated to be $4.1 \times 10^{16} m^{-2}$, i.e. the value which is 5 to 7 orders of magnitude greater than the values calculated from the creep data using one structure parameter only, namely the particle radius r.

Now, let us return to Fig. 6. Along the σ/σ_d ratio vs. T curve for any value of $\dot{\varepsilon}_m / D_L$ under consideration, the stress σ decreases. Thus, for instance, along the curve for $\dot{\varepsilon}_m / D_L = 5 \times 10^9 m^{-2}$, the stress σ decreases from 202.4 MPa at 823 K to 111.3 MPa at 923 K (Fig. 5). The opposite holds for the relaxation factor k_R, Fig. 7. Along the k_R vs. T curve for the same value of $\dot{\varepsilon}_m / D_L$, i.e. $5 \times 10^9 s^{-2}$ the factor k_R increases from 0.918 at the stress 202.4 MPa to 0.954 at the stress of 111.3 MPa. This is why in Figs. 6 and 7 the curves for two different applied stress values, namely 202.4 MPa and 175.9 MPa, are shown. Vertical distances between these two curves at any given temperature illustrate the effect of stress on σ/σ_d and k_R, respectively. This effect need not be considered significant except, perhaps, for temperatures above 873.

Similar "isostress" curves are shown in Fig. 8, in which the relations between the structure factor C for both values of $\dot{\varepsilon}_m / D_L$ under consideration are presented.

According to eqn. (3), the detachment stress σ_d should scale with the shear modulus, since the Orowan bowing stress is proportional to this modulus. However, the σ_d/G ratio decreases with increasing temperature, Fig. 9. Further, the Orowan bowing stress σ_o, calculated by means of eqn. (3) using the values of σ_d and k_R presented in Figs. 6 and 7, are unrealistically high. Thus, for $\dot{\varepsilon}_m / D_L = 5 \times 10^9 m^{-2}$ the calculated σ_o increases from 380 MPa at 923 K to 514 at 823 K and for $\dot{\varepsilon}_m / D_L = 5 \times 10^{11} m^{-2}$ from 565 MPa at the former to 643 MPa at the latter temperature. For comparison, the yield stress values at the above temperatures were estimated correcting the room temperature yield stress (σ_y = 560 MPa /2/) for the temperature dependence of shear modulus. The yield stress amounts to 399 MPa at 923 K and 419 MPa at 823 K.

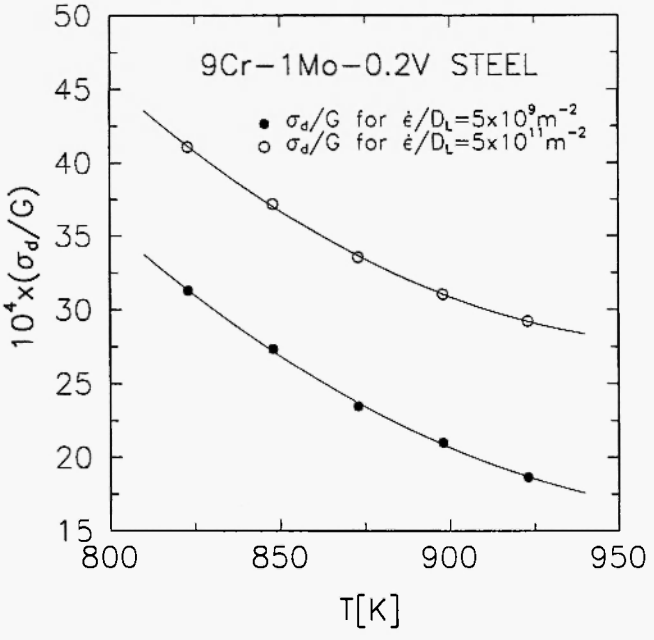

Fig. 9: Relations between σ_d/G and temperature for the $\dot{\varepsilon}_m / D_L$ values under consideration.

From the above analysis it follows that the Rösler-Arzt model /6/ cannot account for the experimental data of interest in the present paper. Nevertheless, following these authors, the $\dot{\varepsilon}_m / D_L$ vs. σ/G relations calculated from the values of k_R, σ_d/σ and C using the particle radins r are compared with the experimental data in Fig. 10. The values of k_R, σ_d/σ and C used in the calculation represent these quantities averaged for $\dot{\varepsilon}_m / D_L$ equal to $5 \times 10^9 m^{-2}$ and $5 \times 10^{11} m^{-2}$ at the temperature of 873 K. The agreement of the model with the experiment is evidently not satisfactory. The value of structure factor C used in the correlation is six orders of magnitude smaller than that calculated from the structure data. When the value of C following from the structure data, namely $4.1 \times 10^{16} m^{-2}$ (see above) is applied, the disagreement of the model with experimental data is still more violent, Fig. 10.

In this connection, it may not be inappropriate to point out that from the results of correlation of creep data for aluminium and aluminium alloys strengthened by aluminium carbide particles /7/, it cannot be concluded that the Rösler-Arzt model /6/ accounts satisfactorily for the stress, but not for the temperature dependence of the minimum creep strain /7/. In fact, the apparent stress exponent m_c is related to the apparent activation energy of creep Q_c through the identity (e.g. /2/)

$$[\partial m_c / \partial (-1/RT)]_\sigma = (\partial Q_c / \partial \ln \sigma)_T \qquad (8)$$

Hence, when the model cannot properly account for the temperature dependence of the minimum creep strain rate, its accounting for the stress dependence of this creep strain rate cannot, in itself, be taken as supporting that model.; a similar conclusion holds true when the model cannot account for the stress dependence of minimum creep strain rate.

4. TIME TO CREEP FRACTURE

The relations between time to creep fracture t_f and applied stress σ for five temperatures ranging from 823 K to 923 K are presented in the paper by Sklenička *et al.* /1/. The times to creep fracture cover six orders of

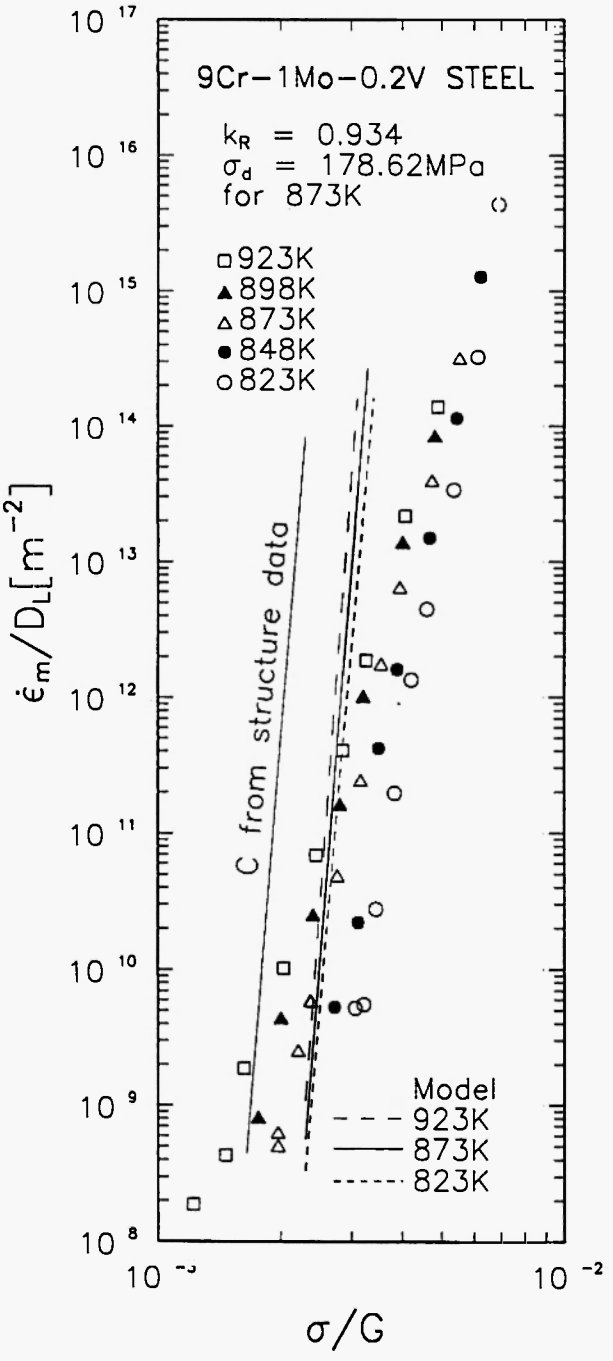

Fig. 10: Correlation of Rösler and Arzt's model with experimental creep data. The mean values of k_R, σ_d and C for a temperature 873K are used and only the data for temperatures 823K, 873K and 923K are considered. In the figure, the $\dot{\varepsilon}_m / D_L$ vs σ/G relation is also shown, obtained using the value of structure factor C calculated from structure data, i.e. ρ, λ and b.

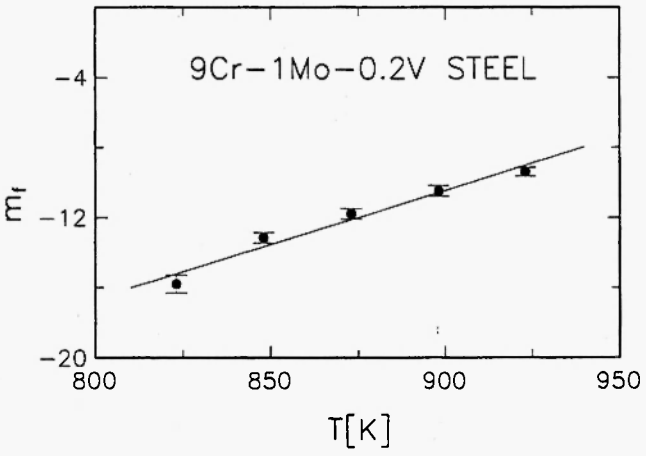

Fig. 11: Temperature dependence of the apparent stress exponent m_f. This exponent does not depend on applied stress σ and can be described as $m_f = 42.07\text{-}472221/T$.

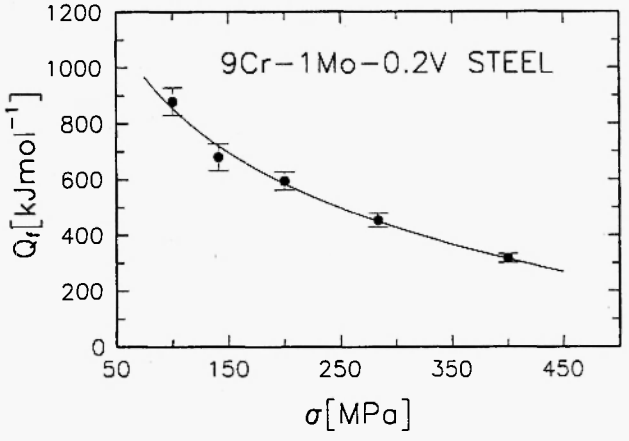

Fig. 12: Stress dependence of the apparent activation energy of time to creep fracture Q_f. The energy Q_f does not depend on temperature and can be described as Q_f [kJmol^{-1}] = 2644.7 - 388.91nσ.

magnitude. The relations under consideration need not be reproduced here. On the other hand, the apparent stress exponent of (time to) fracture

$$m_f = (\partial \ln t_f / \partial \ln \sigma)_T \qquad (9)$$

and the apparent activation energy of (time to) fracture

$$Q_f = [(\partial \ln t_f / \partial(-1/RT)]_\sigma \qquad (10)$$

obtained as functions of temperature and applied stress, respectively, from the creep fracture data /1/ of interest here, are shown in Figs. 11 and 12. The relations $m_f(T)$

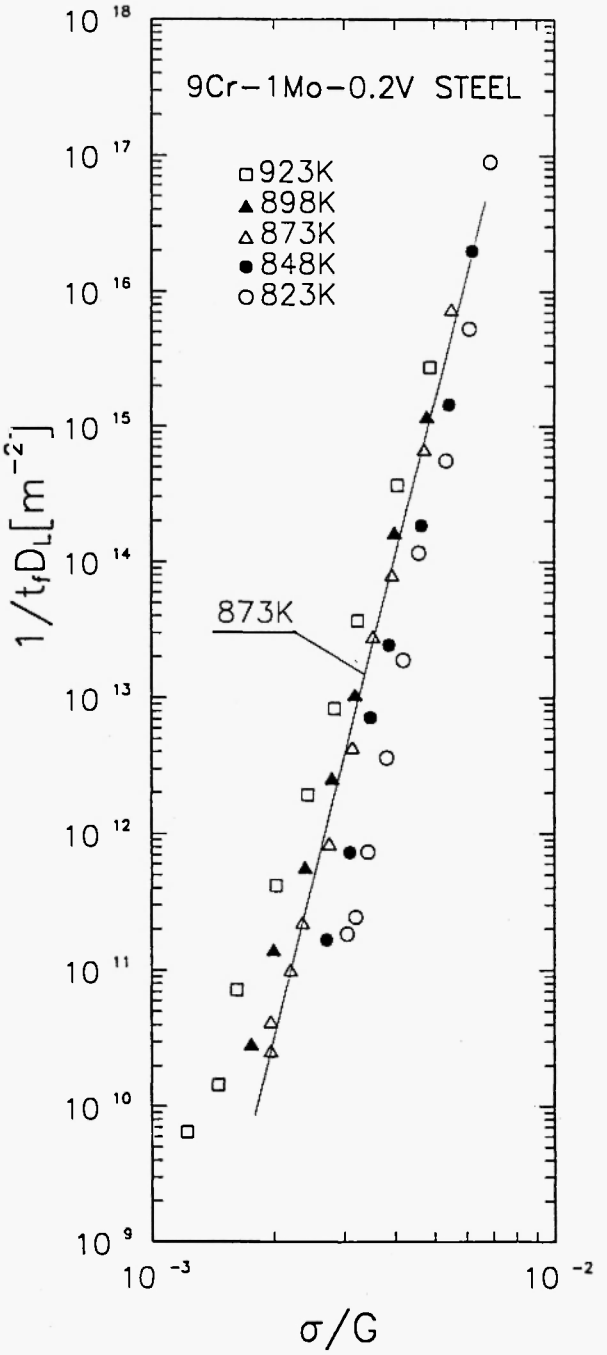

Fig. 13: The times to creep fracture normalized to the lattice diffusion coefficient, $1/t_f D_L$ plotted against stress normalized to the shear modulus, σ/G. The data points do not fit a single curve in the figure, only the curve for 873L is shown.

and $Q_f(\sigma)$ are very similar to the relations $m_c(T)$ and $Q_c(\sigma)$, respectively, although $m_f(T)$ is slightly smaller and $Q_f(\sigma)$ slightly higher than the corresponding parameters for creep. This is probably due to a temperature and stress dependence of creep strain to fracture ε_{cf}.

In Fig. 13, the times to creep fracture normalized to the coefficient of lattice diffusion, $1/t_f D_L$, are plotted against applied stresses normalized to the shear modulus, σ/G. The data points do not fit a single curve; only the straight line for a temperature 873 K is shown in the figure. Hence the picture is essentially the same as in the case of the normalized minimum creep strain rates, $\dot{\varepsilon}_m / D_L$, plotted against applied stresses normalized to the shear modulus σ/G, Fig. 4. Figure 13 suggests, quite strongly, that the time to creep fracture is not lattice diffusion controlled.

4.1. Time-to-Fracture Controlling Process

The results presented in the previous section suggest that the time to creep fracture is controlled by the same process and/or dislocation mechanism as the minimum creep strain rate. This suggestion is further supported by the result of Sklenička *et al.* /1/; these authors showed that the well known Monkman-Grant /8/ relationship $\dot{\varepsilon}_m / t_f = \text{const.}$ holds.

In Fig. 14, the Monkman-Grant relationship modified introducing the creep strain to fracture /9/ is shown. In the figure, values of $\dot{\varepsilon}_{cf} / t_f$ are plotted against the minimum creep strain rates $\dot{\varepsilon}_m$ in double logarithmic coordinates. The slope of the strain line in these coordinates, the exponent p, is almost exactly equal to 1 (in fact $p = 0.9804 \pm 0.066$) so that the Monkman-Grant relationship can be expressed as

$$\varepsilon_{cf} / t_f = \dot{\varepsilon}_m^p \quad ; p \cong 1 \tag{11}$$

It is worth pointing out here that the exponent $p \cong 1$ is observed very frequently in creep fracture experiments with polycrystals, independently of whether fracture is transgranular (as is the case of 9Cr-1Mo-0.2V steel) or intergranular. This strongly suggests that the fracture is constrained /10,11/.

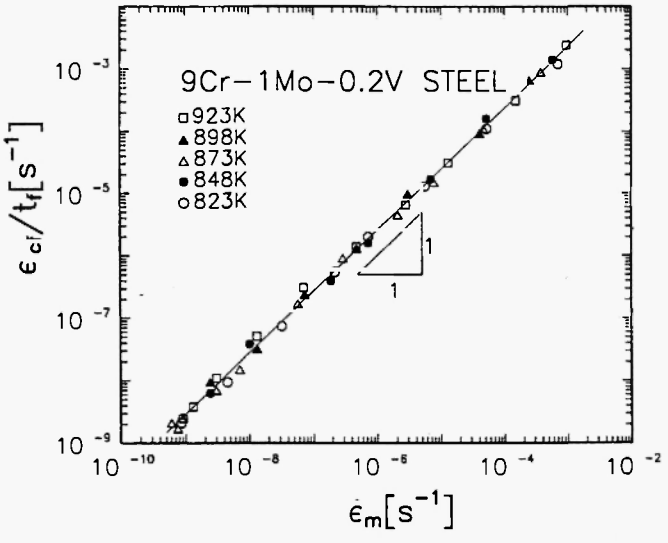

Fig. 14: Relation between ε_{cf}/t_f (ε_{cf} is the creep strain to fracture) and the minimum creep strain rate in double logarithmic coordinates. The relation can be described as: $\ln(\varepsilon_{cf}/t_f) = A + p \ln \dot{\varepsilon}_m$, where $A = 0.671 \pm 0.104$, $p = 0.9804 \pm 0.066$, regression coefficient $r = 0.9990$.

5. DISCUSSION

5.1. Creep

The most striking feature of the creep in the steel of interest in the present paper is very strong temperature dependence of the apparent stress exponent m_c and, correspondingly (see eqn. (8)), very strong stress dependence of the apparent activation energy of creep Q_c. Even when corrected for the temperature dependence of shear modulus, the activation energy of creep is much higher than the activation enthalpy of lattice diffusion ΔH_L, at least at low stresses (see Fig. 4). Thus, any attempt to develop a model of creep in the steel under consideration must necessarily take the above features into account.

Since the minimum creep strain rate is not lattice diffusion controlled, the recovery involving climb of dislocations and their annihilation as well as the climb of dislocations past carbide particles can be excluded as possible creep strain rate controlling mechanisms, provided any dislocation/particle interaction can be disregarded. However, the interaction of dislocations with carbide particles may be "attractive" in nature,

since the $M_{23}C_6$ type carbide particles are not coherent or semicoherent with the steel matrix. This possibility has been taken into account in the above analysis (Section 3). The analysis has led to the conclusion that the Rösler-Arzt model /6/, assuming an attractive interaction of dislocation with dispersed particles and thermally activated detachment of the dislocations from particles, fails to account for the experimental data /1/ considered in the present paper. This can be explained either by (i) very weak, if any dislocation/particle interaction. But then the creep strain rate should be expected to be lattice diffusion controlled (i.e. controlled by dislocation climb past "noninteracting" particles, or by recovery); or (ii) by the Rösler-Arzt model being not properly formulated. Of course, the structure instability may also play a role in creep of the steel of interest, although this cannot explain the above-mentioned $m_c(T)$ and $Q_c(\sigma)$ relations.

Sklenička *et al.* /1/ suggested the role of dislocation substructure changes to dominate the role of precipitation strengthening due to carbide particles. According to these authors, the carbide particles merely stabilize the substructure, though perhaps relatively slightly. But it is the dislocation structure and/or substructure behaviour that determines the above creep characteristics of the steel of interest /1/.

5.2. Creep Fracture

Sklenička *et al.* /1/ concluded that "both the deformation and fracture are controlled by the same mechanism" in creep of the 9C-1Mo-0.2V steel under consideration. The results of the present analysis seem to show quite convincingly that this mechanism is not (directly) dependent on lattice diffusion. At the same time, the results mentioned strongly suggest that the time to creep fracture is not dependent on thermally activated detachment of dislocations from carbide particles – the process for which an activation energy higher than the activation enthalpy of lattice diffusion ΔH_L should be expected.

6. SUMMARY AND CONCLUSIONS

A remarkably extensive set of creep and creep fracture data for a 9Cr-1Mo-0.2V (P91 type) steel /1/ is analyzed in an attempt to account for an unusual stress and temperature dependence of both the creep strain rate and the time to creep fracture. The analysis suggests that the creep strain rate is not recovery controlled, neither is the dislocation climb past non-interacting particles controlled. Also, the model of thermally activated detachment of dislocations from particles fails to account for the stress and temperature dependence of creep strain rate. Thus the carbide particles, probably, play an indirect role affecting the development of dislocation substructure in the course of creep and, especially, the effect of stress and temperature on its parameters. This is in accordance with the original suggestion of Sklenička *et al.* /1/.

Everything that holds for creep strain rate also holds for time to creep fracture. In fact, the time to creep fracture is most probably controlled by the same process and/or mechanism as creep in the 9Cr-1Mo-0.2V steel as originally suggested by Sklenička.

As already mentioned, Sklenička *et al.* /1/ emphasized the role of dislocation substructure behaviour to dominate the role of precipitation strengthening due to carbide particles. According to these authors, the carbide particles stabilize the dislocation substructure, though perhaps rather slightly. But it is the dislocation structure and/or substructure behaviour that determines the creep characteristics of the 9Cr-1Mo-0.2V steel of interest and the same obviously holds for time to creep fracture.

Thus, it seems likely that the model to be developed to account for creep as well as creep fracture behaviour of the 9Cr-1Mo-0.2V steel should take into account the subgrain structure and its changes with both the stress and temperature in creep, perhaps along a line similar to that recently developed by Dobeš *et al.* /12/, re-analysing the creep behaviour of mechanically alloyed aluminium and some aluminium alloys strengthened by aluminium carbide and aluminium oxide particles.

ACKNOWLEDGEMENTS

The authors wish to thank Drs. V. Sklenička and K. Kucharová for valuable discussions and Mrs. M. Pichová for assistance in manuscript preparation. Financial support from the Grant Agency of the Czech

Republic under the Grant 106/96/0322 is greatly appreciated.

REFERENCES

1. V. Sklenička, K. Kuchařová, A. Dlouhý and J. Krejči, in: *Proc. Conf. Materials for Advanced Power Engineering 1994*, D. Coutsourdis *et al.* (Eds.). Kluwer Academic Publishers, Dordrecht, 1994; p. 435.
2. J. Čadek , *Creep in Metallic Materials*, Elsevier, Amsterdam, 1988; p. 90.
3. J. Čadek , V. Šustek and M. Pahutová, to be published.
4. J. Rösler and E. Arzt, *Acta Metall.*, **36**, 1043 (1988).
5. E. Arzt and D.S. Wilkinson, *Acta Metall.*, **34**, 1893 (1986).
6. J. Rösler and E. Arzt, *Acta Metall. Mater.*, **38**, 671 (1990).
7. A. Orlová and J. Čadek , *Acta Metall. Mater.*, **40**, 1865 (1992).
8. F.C. Monkman and N.J. Grant, *Proc. ASTM*, **56**, 593 (1956).
9. F. Dobeš and K. Milička, *Met. Sci.*, **10**, 382 (1976).
10. H. Riedel, *Fracture at High Temperatures*, Springer-Verlag, Berlin, 1987; p. 172.
11. J. Čadek , *Mater. Sci. Eng.*, **A117**, L5 (1989).
12. F. Dobeš, K. Kuchařová, A. Orlová, K. Milicka and J. Čadek , *Acta Metall. Mater.*, **42**, 1447 (1994).